

- Charney JI and Alexander LM (1991) *International Maritime Boundaries*. Boston: Martinus Nijhoff.
- Churchill RR and Lowe AV (1988) *The Law of the Sea*. Manchester: Manchester University Press.
- D'Amato A and Engel K (1996) *International Environmental Law Anthology*. Cincinnati: Anderson.
- Food and Agriculture Organization (2000) www.fao.org.
- Group of Experts on the Scientific Aspects of Marine Pollution (1990) *The State of the Marine Environment*. UNEP Regional Seas Reports and Studies, No. 115. Nairobi: United Nations Environment Programme.
- International Maritime Organization (2000) Summary of status of conventions as at 31 July 2000. www.imo.org/imo/convent/summary.htm.
- Joyner CC (2000) The international ocean regime at the new millennium: a survey of the contemporary legal order. *Ocean and Coastal Management* 43: 163–203.
- Schoenbaum TJ (1994) *Admiralty and Maritime Law*, 2nd edn, Vol. 1. St Paul: West Publishing.
- United Nations Law of the Sea (2000) www.un.org/Depts/los.htm.
- United Nations Secretary General (1989) Law of the sea: protection and preservation of the marine environment. *Report of the Secretary General A/44/461*.

## LEEUWIN CURRENT

See **INDONESIAN THROUGHFLOW AND LEEUWIN CURRENT**

## LONG-TERM TRACER CHANGES

**F. von Blanckenburg**, Universität Bern, Bern, Switzerland

Copyright © 2001 Academic Press

doi:10.1006/rwos.2001.0175

### Introduction

Ocean tracers that record long-term changes preserve certain water column information within the sediment. This information comprises (1) the tracers' fluxes in the past, such as erosional input from the continents, hydrothermal activity at mid-ocean ridges, input of extraterrestrial material, or carbonate recycling; (2) the distribution of water masses in the past and the state of the past global thermohaline circulation. Inorganic isotope tracers whose isotope ratios are modified by radioactive decay in their source materials are ideally suited for these studies. Their original water column values can be measured in materials such as biogenic carbonates, ferromanganese crusts and nodules, and the authigenic phase of deep-sea sediments.

Studies of tracer fluxes in the past are favored by those tracers whose residence time in the ocean ( $\tau$ , defined below) is long relative to the turnover time of the thermohaline circulation (1500 y), such as Sr and Os. Tracers of which  $\tau$  is of the order of, or shorter than the oceans turnover time (Nd, Hf, Pb, Be) offer the ability to label water masses isotopi-

cally. In this case, long-term isotope changes of these intermediate- $\tau$  tracers are potentially caused by variations of the thermohaline circulation. However, secular variations of these isotope tracers can also be caused by regional variations in these tracers' fluxes, mostly resulting from changes in weathering. It is not always straightforward to distinguish between these two causes of tracer variations.

Certainly the globally uniform seawater isotope evolution of Sr, Os, and potentially also Be, offer excellent tools for isotope stratigraphy on long (My) timescales.

### Definitions and Concepts

Long-term tracers are those elements whose isotopic compositions provide information on the physical and chemical state of the oceans on timescales of several thousands of years to millions of years (My). For example, paleo-oceanographers aim to reconstruct past water mass distributions and the mode of the thermohaline circulation. For this purpose it would be desirable to reconstruct past oceanographic water mass characteristics such as salinity, temperature, silica, or phosphorus content from the sedimentary record. Similarly, the reconstruction of the past land-sea transfer of certain tracers is desirable in order to reconstruct changes in the weathering history of the continents. However, these

present-day tracers are usually not conserved in the sedimentary record. Even if they were precipitated chemically and stored in sediments, their changes in concentration as measured in a sedimentary column back through time cannot be directly related to past water mass properties. This is because the tracers' concentrations in sediments depend on factors such as sedimentation rate, diagenesis, partitioning into a certain phase, uptake by organisms, and additions of the same element by detrital hemipelagic or aeolian material. Therefore ocean chemists make use of proxy tracers which are not routinely analyzed in surveys of present-day water masses, because their measurement presents a considerable effort compared with tracers such as salinity and temperature. However, their characteristics can be directly related to those well-known oceanographic seawater tracers.

The conditions that need to be met for an element to be of use as a proxy tracer are that (1) it conserves a characteristic chemical or isotopic property when transferred from the water column into the sediment; (2) the elements or their isotopic composition can be extracted from the sediment; (3) the age of the sediment is known so that changes of the tracer over time can be reconstructed.

One such proxy makes use of element ratios. For example, the ratio of Cd to Ca in foraminiferal tests is a proxy for the  $\text{PO}_4$  content of the past water mass in which the foraminifera formed and therefore provides information on the past thermohaline circulation. This tracer is explained in detail in the article on trace elements in foraminiferal tests. Similarly, the ratio of the intermediate uranium decay products  $^{231}\text{Pa}$  and  $^{230}\text{Th}$ , measured in bulk sediment, may under certain conditions provide information on the advection of water masses in the overlying water column in the past (*see Cosmogenic Isotopes and Uranium–Thorium Series Isotopes in the Ocean.*) Isotope ratios are ideally suited as long-term proxy tracers. Some of these isotope ratios are characteristic of certain seawater properties and can be measured in sediments, regardless of the actual tracer partitioning, concentration, or location of precipitation.

A property describing the behavior of a tracer in sea water is the residence time  $\tau$ . If the tracer's fluxes in and out of an ocean basin are invariant with time, the tracer is at steady state and the residence time can be calculated from the tracer's ocean inventory:

$$\tau = \frac{\text{Inventory}}{\text{Flux}_{\text{in}}} = \frac{\text{Inventory}}{\text{Flux}_{\text{out}}}$$

A tracer suitable as a water mass tracer has a short global residence time ( $\tau$ ) relative to the ocean's

mixing time. This ensures that isotope 'fingerprints' characteristic of a certain water mass are prevented from being completely dispersed by the global thermohaline circulation. While the global ocean mixing time is difficult to assess, a meaningful quantity is the time it takes for one turnover of the global deep water circulation, which is c. 1500 y. Tracers with  $\tau$  of this order have the potential to preserve distinct water mass labels. It can be assumed that a conservative (i.e. nonreactive) tracer would be almost perfectly homogenized within 10 000–20 000 years. Tracers with  $\tau$  in excess of this period will only record changes in the global flux of this tracer, regardless of the water mass, the location of the input, or the location of the samples taken.

### Isotope Tracers Used

Much use is made of the stable isotopes of carbon as a paleo-water mass isotope 'fingerprint'. The  $^{13}\text{C}/^{12}\text{C}$  ratio in the tests of foraminifera depends on the relative position of the overlying water mass within the thermohaline circulation system. However, these isotope ratios are modified during the incorporation into organisms, depend on availability of nutrients, and like the isotopes of oxygen, also depend on seawater temperature. (These tracers are dealt with in the relevant articles; please refer to the See also section.)

Isotope ratios of inorganic trace metals which are the topic of this chapter are not modified when incorporated into the sediment (note that some minor isotope fractionation might occur on incorporation into the sediment, but usually such shifts are either smaller than analytical precision or they are removed by the internal correction procedures of the techniques used). The variation in isotope ratios only varies by radioactive decay of the parent isotope of at least one isotope in the tracer's sources or cosmogenic production. The elements currently in use for paleo-oceanography are given in **Table 1**.

As apparent from the properties listed in **Table 1**, ocean chemists have a variety of tracers at hand, covering a range of residence times and chemical behaviors. Those tracers varying due to radioactive decay have distinct isotopic compositions in their various source materials (**Table 2**). This makes them particularly useful both as water mass tracers, and to reconstruct the flux from these various sources into the oceans. It may be surprising to find the cosmogenic nuclide  $^{10}\text{Be}$  in this list of otherwise radiogenic tracers. The reason is that Be behaves very similarly to the other tracers in that the ratio  $^{10}\text{Be}/^9\text{Be}$  is distinct in different water masses. Given that  $^{10}\text{Be}$  is the only tracer of which the flux into the

**Table 1** Long-term isotope tracers currently in use

Tracer	Isotopes	Sources	Average deep-water concentration	Global deep-water residence time
Strontium (Sr)	<sup>87</sup> Sr (stable) ← <sup>87</sup> Rb ( <i>T</i> <sub>1/2</sub> = 48.8 Gy) <sup>86</sup> Sr (stable, primordial)	Mostly chemical weathering of the continental crust and carbonates Hydrothermal solutions from mid-ocean ridges Dissolution of marine carbonates	7.6 μg g <sup>-1</sup>	2–4 My
Osmium (Os)	<sup>187</sup> Os (stable) ← <sup>187</sup> Re ( <i>T</i> <sub>1/2</sub> = 43 Gy) <sup>188</sup> Os (stable, primordial)	Erosion of the continental crust (chemical weathering important) Leaching of abyssal peridotites Cosmic dust and spherules	10 fg g <sup>-1</sup>	8000–40 000 y
Neodymium (Nd)	<sup>143</sup> Nd (stable) ← <sup>147</sup> Sm ( <i>T</i> <sub>1/2</sub> = 106 Gy) <sup>144</sup> Nd (stable, primordial)	Erosion of the continental crust	4 pg g <sup>-1</sup>	~ 1000–2000 y
Hafnium (Hf)	<sup>176</sup> Hf (stable) ← <sup>177</sup> Lu ( <i>T</i> <sub>1/2</sub> = 37.3 Gy) <sup>177</sup> Hf (stable, primordial)	Erosion of the continental crust Hydrothermal solutions at mid-ocean ridges	0.18 pg g <sup>-1</sup>	~ 1000–2000 y?
Lead (Pb)	<sup>208</sup> Pb (stable) ← <sup>232</sup> Th ( <i>T</i> <sub>1/2</sub> = 14.0 Gy) <sup>207</sup> Pb (stable) ← <sup>235</sup> U ( <i>T</i> <sub>1/2</sub> = 0.704 Gy) <sup>206</sup> Pb (stable) ← <sup>238</sup> U ( <i>T</i> <sub>1/2</sub> = 4.47 Gy) <sup>204</sup> Pb (stable, primordial)	Erosion of the continental crust Hydrothermal solutions at mid-ocean ridges (minor) Today: industrial Pb	1 pg g <sup>-1</sup>	40 y (Atlantic) 80–200 y (Pacific)
Be	<sup>10</sup> Be (cosmogenic, <i>T</i> <sub>1/2</sub> = 1.5 My)	<sup>10</sup> Be: atmospheric precipitation by rain	1000 atoms/g	250 y (Atlantic)
Beryllium	<sup>9</sup> Be (stable, primordial)	<sup>9</sup> Be: erosion of the continental crust	0.25 pg g <sup>-1</sup>	600 y (Pacific)

**Table 2** Isotope ratios of source materials

Isotope ratio	Pacific mid-ocean ridges	Average upper continental crust	Cosmic dust
<sup>87</sup> Sr/ <sup>86</sup> Sr	0.7028	0.72	N/A
<sup>187</sup> Os/ <sup>188</sup> Os	0.125 (abyssal peridotites)	1.26	0.126
<sup>143</sup> Nd/ <sup>144</sup> Nd	0.5132	0.5121	
$\epsilon_{\text{Nd}}$	+10	-11.4	N/A
<sup>176</sup> Hf/ <sup>177</sup> Hf	+20	-10	
$\epsilon_{\text{Nd}}$	0.2834	0.2825	N/A
<sup>206</sup> Pb/ <sup>204</sup> Pb	18.5	19.3	
<sup>207</sup> Pb/ <sup>204</sup> Pb	15.5	15.7	N/A
<sup>208</sup> Pb/ <sup>204</sup> Pb	38.0	39.1	

$\epsilon_{\text{Nd}}$  and  $\epsilon_{\text{Hf}}$  are <sup>143</sup>Nd/<sup>144</sup>Nd and <sup>176</sup>Hf/<sup>177</sup>Hf ratios, respectively, normalized to a chondritic value CHUR. <sup>143</sup>Nd/<sup>144</sup>Nd<sub>CHUR</sub> = 0.512638; <sup>176</sup>Hf/<sup>177</sup>Hf<sub>CHUR</sub> = 0.282772; (N/A): Not Available.

$$\epsilon_{\text{Nd}} = \left( \frac{^{143}\text{Nd}/^{144}\text{Nd}_{\text{sample}}}{^{143}\text{Nd}/^{144}\text{Nd}_{\text{CHUR}}} - 1 \right) * 10^4 \quad \epsilon_{\text{Hf}} = \left( \frac{^{176}\text{Hf}/^{177}\text{Hf}_{\text{sample}}}{^{176}\text{Hf}/^{177}\text{Hf}_{\text{CHUR}}} - 1 \right) * 10^4$$

oceans is known,  $\tau$  can be calculated precisely from its water column concentration. Further, the continent-derived isotope <sup>9</sup>Be is the only tracer of which the flux into the oceans can be calculated from the <sup>10</sup>Be/<sup>9</sup>Be ratio.

Examples of the isotopes of Nd and Be as water mass labels are shown in **Figures 1a and b**. The isotope variations of Nd are so small that the <sup>143</sup>Nd/<sup>144</sup>Nd ratio is reported normalized to a ratio typically found in chondritic meteorites ('CHUR'):

$$\epsilon_{\text{Nd}} = \left( \frac{^{143}\text{Nd}/^{144}\text{Nd}_{\text{sample}}}{^{143}\text{Nd}/^{144}\text{Nd}_{\text{CHUR}}} - 1 \right) \times 10^4$$

The salinity contours in **Figure 1** define water masses, such as North Atlantic Deep Water (NADW), Antarctic Intermediate Water (AAIW), and Antarctic Bottom Water (AABW). Note that  $\epsilon_{\text{Nd}}$  is -13.5 in NADW, and <sup>10</sup>Be/<sup>9</sup>Be is *c.*  $0.5 \times 10^{-7}$ . In the southern circumpolar water  $\epsilon_{\text{Nd}}$  is -9, and <sup>10</sup>Be/<sup>9</sup>Be is  $1 \times 10^{-7}$ . <sup>10</sup>Be/<sup>9</sup>Be, and in particular  $\epsilon_{\text{Nd}}$ , mimic the shape of salinity. Incorporation of these tracers into

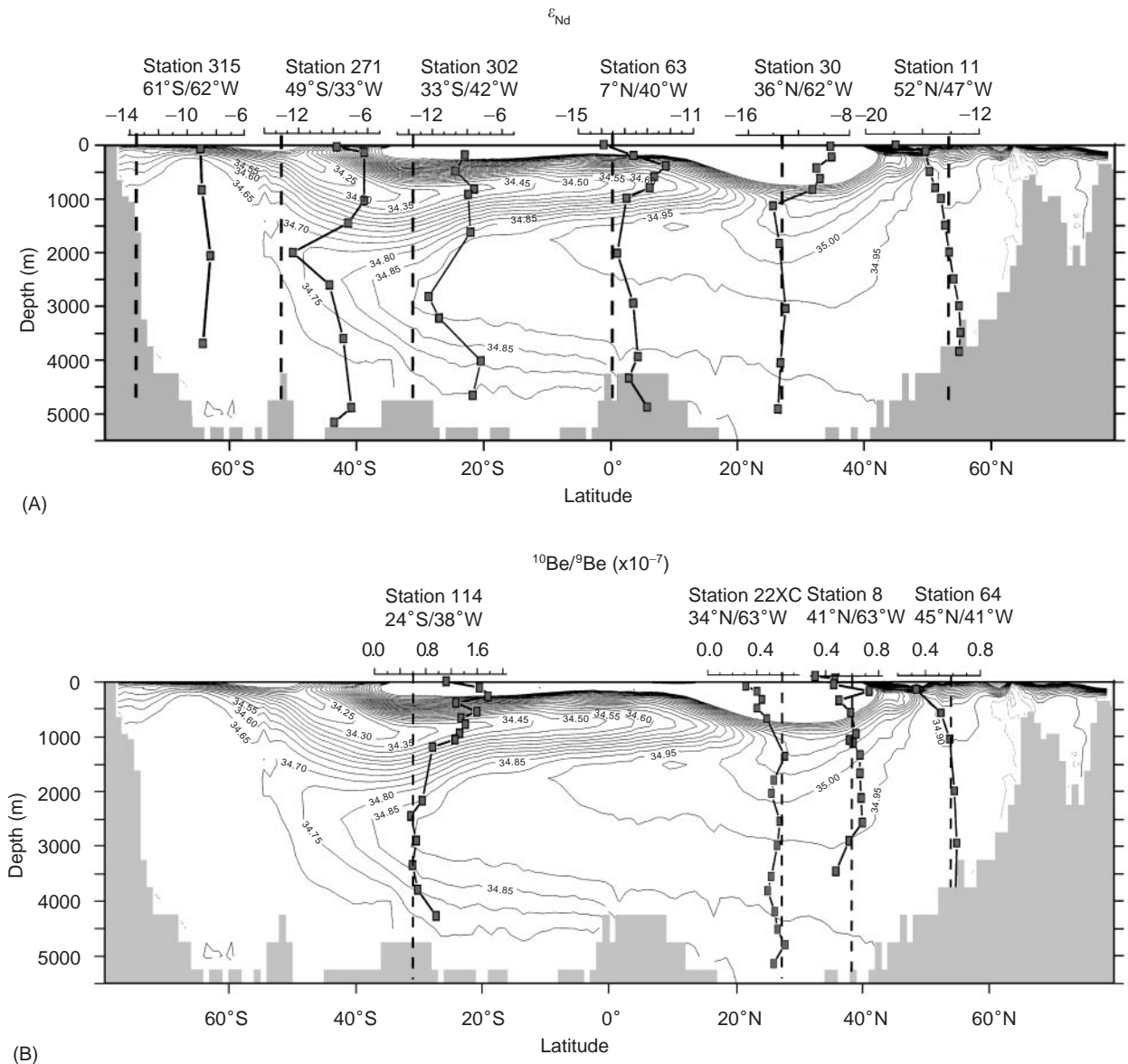


**Figure 1** (A) Salinity contours of Atlantic sea water with superimposed dissolved Nd isotope compositions. Stippled line gives the typical composition of NADW ( $\epsilon_{Nd} = -13$ ). Note the pronounced tongue of NADW with intermediate salinities and  $\epsilon_{Nd}$  of  $-13$  spreading south, and the tongues of AABW and AAIW with lower salinities and  $\epsilon_{Nd}$  of  $-9$  spreading north. (Reprinted with permission from von Blanckenburg F (1999) Tracing past ocean circulation? *Science* 286: 1862–1863. Copyright 1999 American Association for the Advancement of Science.) (B) Salinity contours of Atlantic sea water with superimposed dissolved Be isotope compositions. Stippled line gives the typical composition of NADW ( $^{10}Be/^{9}Be = 0.6 \times 10^{-7}$ ). Note the pronounced tongue of AAIW with lower salinities and  $^{10}Be/^{9}Be$  of  $1 \times 10^{-7}$  spreading north. (Data reproduced with permission from Ku *et al.*, 1990; Xu, 1994; Measures *et al.*, 1996).

the sediment at a given location potentially provides information on the distribution and mixing of water masses at this location back through time.

The schematic global distribution of deep-water isotope ratios of all tracers discussed here is shown in **Figure 2A–F**. Note that the variability decreases with increasing residence time.  $^{87}Sr/^{86}Sr$  is perfectly homogenized (**Figure 2A**). The only location worldwide at which a different Sr isotope ratio has been

measured in sea water is the restricted Baltic Sea, where riverine dilution halves the open-ocean salinity and leads to a distinct  $^{87}Sr/^{86}Sr$  only just detectable by modern analytical methods.  $^{187}Os/^{188}Os$ , with an estimated  $\tau$  of 8000–40000 y, shows only a minute difference between the Atlantic and the other oceans (**Figure 2B**). In contrast, the shorter residence time tracers (Pb, Be, Nd, Hf) show clear gradients between Atlantic and Pacific deep water.

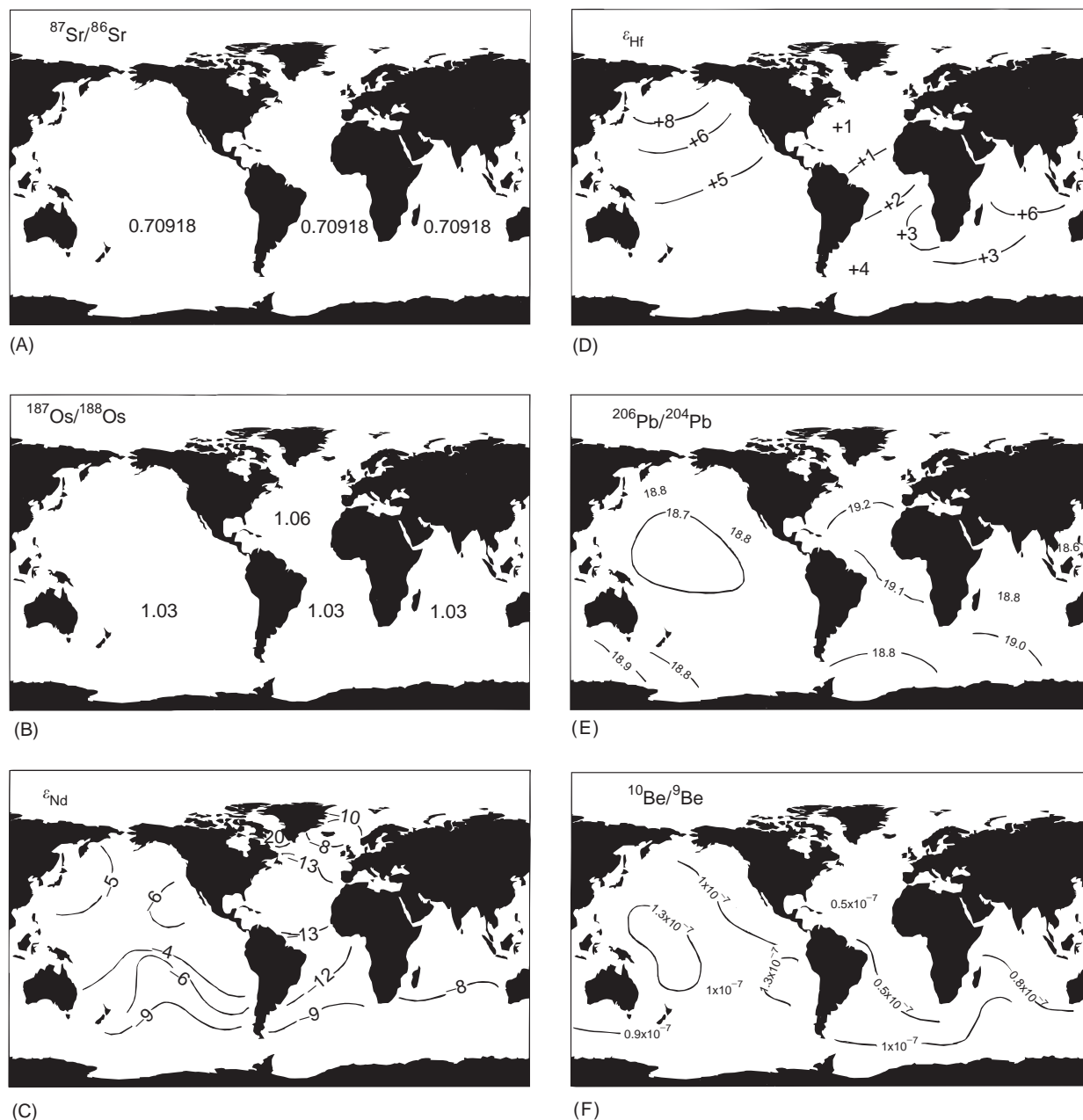


**Figure 2** (A) Map of modern  $^{87}\text{Sr}/^{86}\text{Sr}$  ratios in sea water (relative to 0.710248 for the Sr isotope standard SRM 987 (McArthur, 1994). Note that the long  $\tau$  of Sr (several My) allows for perfect homogenization and uniform isotope ratios in all basins. (B)  $^{187}\text{Os}/^{188}\text{Os}$  isotope ratios in modern sea water as measured on the surface of hydrogenous Fe-Mn crusts (Burton *et al.*, 1999b).  $\tau$  of a few tens of thousands of years just allows for a small difference between the North Atlantic (with its rich input of old continental material) and the other oceans. (C) Dissolved Nd isotope compositions in modern deep sea water as measured in Mn nodules (reproduced with permission from Albarède and Goldstein, 1992), adjusted for more recent measurements of Nd in deep sea water (see references in von Blanckenburg, 1999). A  $\tau$  of c. 1000y allows for distinct gradients between basins, depending on the age and Sm/Nd ratio of their surrounding continental erosion sources. (D)  $\epsilon_{\text{Hf}}$  measured in the surface layer of hydrogenetic Fe-Mn crusts and nodules (Albarède *et al.*, 1998). Similar to Nd, distinct gradients exist between basins. (E) Pre-anthropogenic  $^{206}\text{Pb}/^{204}\text{Pb}$  ratios measured in the surface layer of hydrogenetic Fe-Mn crusts and nodules. (Abouchami and Goldstein, 1995. Reprinted from *Geochimica et Cosmochimica Acta*, 60, von Blanckenburg F, O'Nions RK, Hein JR, Distribution and sources of pre-anthropogenic lead isotopes in deep ocean water as derived from Fe-Mn crust, 4957–4963, Copyright (1996), with permission from Elsevier Science.). Pre-anthropogenic Pb cannot be measured in modern sea water which is dominated by industrial Pb. The short  $\tau$  (40–200y.) results in distinct signatures between and within basins. (F)  $^{10}\text{Be}/^9\text{Be}$  ratios in modern sea water from both the dissolved phase and the surface layer of hydrogenetic Fe-Mn crusts. (Reprinted from *Earth and Planetary Letters*, 141, von Blanckenburg F, O'Nions RK, Belshaw NS, Gibb A, Hein JR, Global distribution of Beryllium isotopes in deep ocean water as derived from Fe-Mn crusts, 213–226, Copyright (1996) with permission from Elsevier Science.)  $^{10}\text{Be}$  is a cosmogenic nuclide that enters the ocean by precipitation from the atmosphere, whereas  $^9\text{Be}$  is stable and enters the oceans by erosion. The global deep-water  $\tau$  of  $^{10}\text{Be}$  is 600y, allowing for preservation of distinct gradients between the basins.

This is because the Atlantic receives the highest flux of continental erosion products (aeolian dust, river particulate matter, river dissolved matter) per unit open-ocean area. Furthermore, all this material is derived from old continental crust with an isotope composition distinct from younger rocks (Table 2). Labrador Sea water, for example, receives erosion products from Archean cratons with a unique isotope composition. In contrast, the Pacific receives most of its tracer input from the surrounding volcanic arcs, which have isotope compositions different from the continental crust surrounding the Atlantic. The Indian Ocean has ratios intermediate between the Atlantic and the Pacific for all of these tracers. Whether this is due to mixing of Atlantic water masses (advected through the circumpolar current) and Pacific water (advected via the Indonesian throughflow), or due to internal sources unique to the Indian Ocean is currently not known.  $^{10}\text{Be}/^9\text{Be}$  ratios are lower in the Atlantic because the North Atlantic receives a higher flux of terrigenous  $^9\text{Be}$ . This keeps the  $^9\text{Be}$  concentration uniform worldwide, whereas  $^{10}\text{Be}$  increases along the advective flow path as expected from a nutrient-type tracer.

### Materials and Methods used in Long-Term Tracer Studies

It is important that sedimentary materials chosen for long-term tracer studies are true chemical or biogenic precipitates formed in the water column. Con-

tamination by terrestrial detrital material (fine clays from aeolian or hemipelagic sources) and material affected by chemical alteration through diagenetic processes has to be avoided. The isotopes of Sr are usually measured on carbonates or barite, while those of Be, Nd, or Hf are extracted from chemical sediments, such as ferromanganese (Fe-Mn) crusts, manganese nodules, the authigenic phase of deep-sea sediments, or marine phosphorites, argillites, and glauconites.

## Results

### Sr

Sr isotopes represent the best-studied long-term tracer, as well-dated carbonate sequences are readily available, the extraction and analysis is simple, and the long residence time ensures worldwide homogenization. Therefore, a single isotope evolution curve has emerged dating back through the entire Phanerozoic (Figure 3), and at a much higher resolution for the Cenozoic (Figure 4). The curve was time-calibrated using biostratigraphy and, in some cases, geochronology of intercalated ash layers. This makes Sr isotopes a very useful tool for stratigraphy. Ages of high confidence can be determined for those periods where  $^{87}\text{Sr}/^{86}\text{Sr}$  underwent strong changes. For some periods unique ages cannot be assigned. For example, the slope in  $^{87}\text{Sr}/^{86}\text{Sr}$  in the Early Tertiary period is too low to allow for high-resolution stratigraphy.

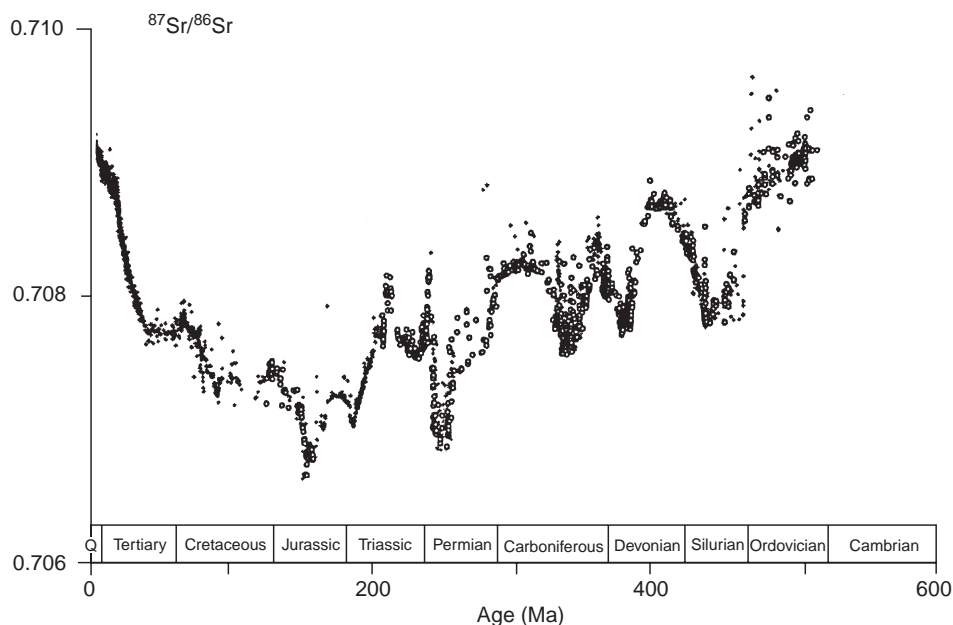


**Figure 3**  $^{87}\text{Sr}/^{86}\text{Sr}$  variations for the Phanerozoicum based on samples of brachiopods, belemnites, conodonts, foraminifera, and samples of micritic matrix. (Adapted from *Chemical Geology*, 161, Veizer J, Ala D, Azmy K *et al.*,  $^{87}\text{Sr}/^{86}\text{Sr}$ ,  $\delta^{13}\text{C}$ ,  $\delta^{18}\text{O}$  evolution of Phanerozoic sea water, 59–88, Copyright (1999), with permission from Elsevier Science.)

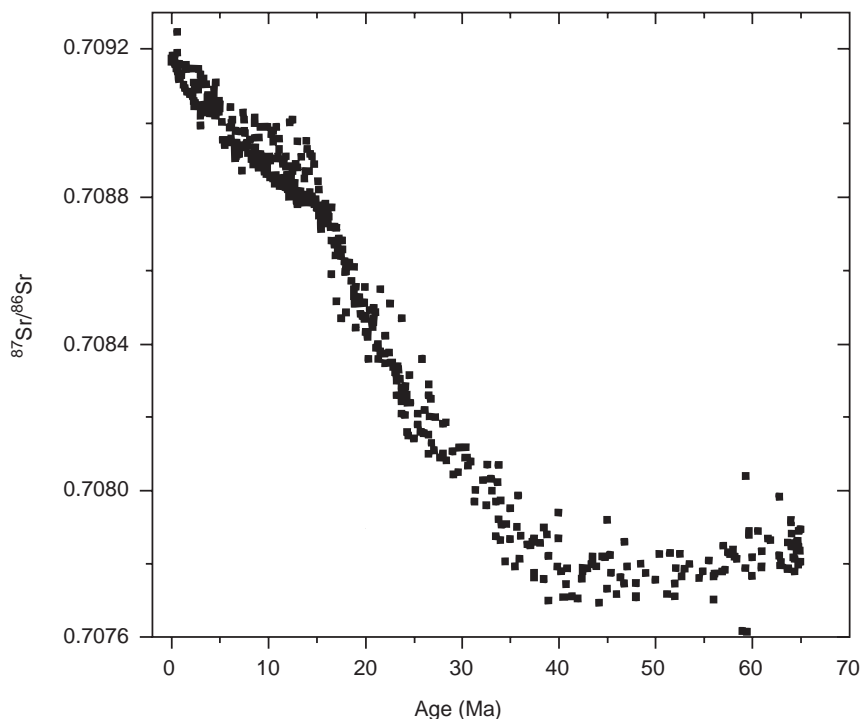


**Figure 4** Cenozoic evolution of marine  $^{87}\text{Sr}/^{86}\text{Sr}$ , based primarily on analyses of foraminifera from all oceans. Data sources are as in McArthur (1994).

The changes in the  $^{87}\text{Sr}/^{86}\text{Sr}$  ratio are controlled by several processes. These are (1) the mid-ocean ridge flux, which is in turn controlled by the spreading rates of the seafloor; (2) the rate of chemical weathering, in particular that of feldspar and calcite; (3) the areal extent of the continents above sea level; (4) changes in the carbonate compensation depth (CCD). Seawater Sr isotope ratios vary within a small range over time. This is because of the long and efficient mixing of Sr, and also because dissolution of continental carbonate buffers seawater Sr isotope compositions within a narrow range.

Some of the trends visible in **Figure 3** are a relatively slow decrease in  $^{87}\text{Sr}/^{86}\text{Sr}$  ratios from the Cambrian to the Jurassic period, upon which are superimposed a number of relatively large fluctuations. The sharp decline and following rise at the Permian/Triassic boundary are spectacular, and are thought to reflect either an extreme climate and weathering change, or the sudden mixing of a previously stratified ocean. A second main trend is a relatively rapid increase in  $^{87}\text{Sr}/^{86}\text{Sr}$  ratios from the Jurassic to the present, upon which a number of relatively small fluctuations are superimposed.

Much discussion has been stimulated by the strong Cenozoic increase in  $^{87}\text{Sr}/^{86}\text{Sr}$  (**Figure 4**) that has been linked by some workers to the uplift of the Himalayas and the ensuing delivery of high  $^{87}\text{Sr}/^{86}\text{Sr}$

by Himalayan rivers. This view was challenged by the recent observation that  $^{187}\text{Os}/^{188}\text{Os}$  (**Figure 5**), showing a similar and simultaneous increase, cannot be attributed to the dissolved flux draining the rising Himalayas. Therefore there must be a different cause for the rise in Sr too, possibly a worldwide increase in weathering rate. Similar attention was focused on the pronounced rise over the past 2.5 My. One possibility is that the latter can be explained simply by changes in sea level during the glaciations. However, calculations have shown that sea level variations of 200–300 m would be required – far in excess of the *c.* 100–150 m of change believed to have taken place during the Quarternary period. Therefore a much more plausible explanation is a change in the terrigenous Sr input supplied by rivers to the oceans. Either a change in the dissolved Sr flux may have occurred or a change in the isotopic composition of rivers, or a combination of both. The increased erosion and availability of weatherable mineral surfaces resulting from the build up of glaciers during the northern hemisphere glaciation might have provided these changes.

#### Os

Because of the exceedingly small differences in  $^{187}\text{Os}/^{188}\text{Os}$  between the different ocean basins, Os has a potential similar to Sr to serve as an isotope

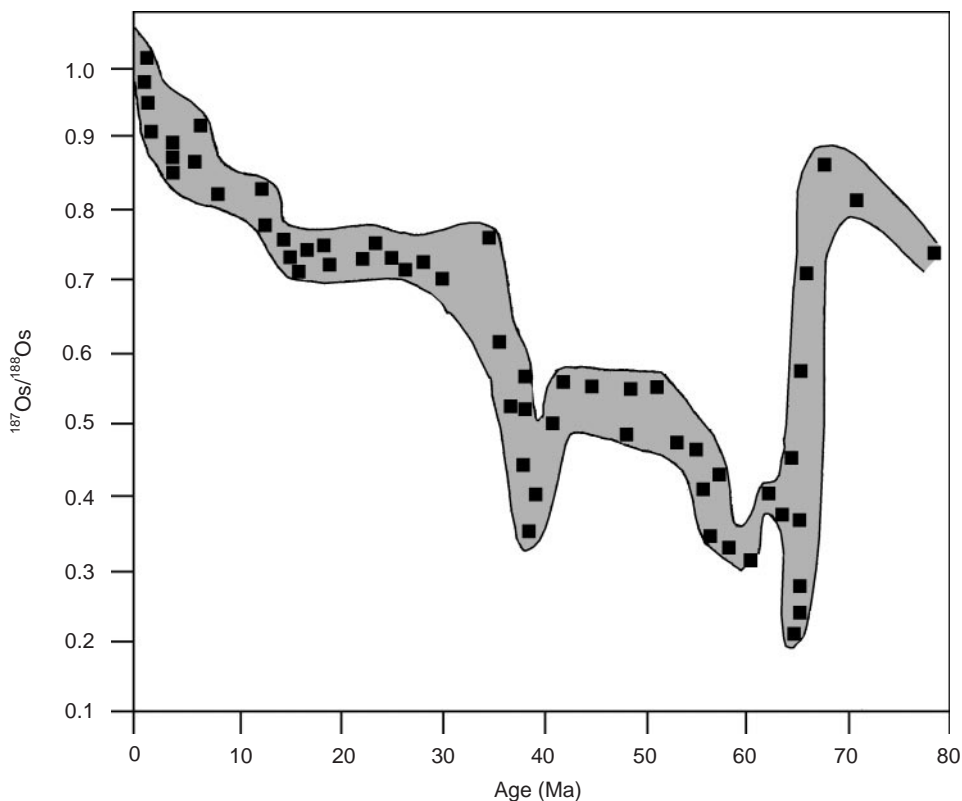


**Figure 5** Marine  $^{187}\text{Os}/^{188}\text{Os}$  record for the past 80 My in all oceans from  $\text{H}_2\text{O}_2$ -leached metalliferous and hydrogenetic sediments. Note that the pronounced excursion to low ratios at the K/T boundary (65 My) is explained by a meteorite impact. (Reprinted from *Geochimica et Cosmochimica Acta*, 63, Pegram WJ, Turekian KK. The osmium isotopic composition change of Cenozoic sea water as inferred from a deep-sea core corrected for meteoritic contributions, 4053–4088, Copyright (1999), with permission from Elsevier Science.)

stratigraphic tool. It is particularly valuable for carbonate-poor pelagic clays and metalliferous sediments, from which Os is extracted by leaching techniques. The Os isotope curve (Figure 5) bears many similarities to the Sr isotope curve (Figure 4), with the exception of three excursions to low  $^{187}\text{Os}/^{188}\text{Os}$  ratios. The spectacular drop at the Cretaceous/Tertiary boundary is probably of meteorite impact origin. The second, mid-Paleocene decrease and also the slow recovery following the impact can be explained by exposure of coastal sediments imprinted by the meteoritic Os from the K/T boundary. The Eocene-Oligocene excursion (~33 Ma) has been explained by an increased supply of nonradiogenic Os from peridotite weathering (Table 2).

As is the case for  $^{87}\text{Sr}/^{86}\text{Sr}$ , there is a strong increase of  $^{187}\text{Os}/^{188}\text{Os}$  towards more radiogenic values over the past ~14 My. As stated above, this has been linked to the rise of the Himalayas, but recent analyses of Himalayan river waters for Os isotope compositions do not support this view.

A more likely possibility is the weathering of ancient crystalline terranes exposed by physical erosion, or the weathering of black shales. These organic-rich sediments have a high Re/Os ratio. Therefore old black shales have the potential to supply Os with a very high  $^{187}\text{Os}/^{188}\text{Os}$  ratio to sea water.

#### Nd

Nd isotopes, analyzed with low-time resolution in Fe-Mn crusts and given as  $\epsilon_{\text{Nd}}$  units, are presented in Figure 6. The most outstanding feature is that the provinciality, observed in  $\epsilon_{\text{Nd}}$  of the modern oceans (Figure 2C), has been a feature prevailing as far back as 55 Ma. It is thought that despite the large isotopic variability in source materials, the  $\tau$  of Nd is sufficiently long to allow for efficient intra-basin homogenization. This produces the basins' characteristic Nd isotope blend. Significant variations in  $\epsilon_{\text{Nd}}$  are mainly observed for the past 5 My. In the Pacific a decrease in  $\epsilon_{\text{Nd}}$  over the past 5 My might be due to an increased flow of AABW (with low  $\epsilon_{\text{Nd}}$ , Figure 2C), a rearrangement of the thermohaline



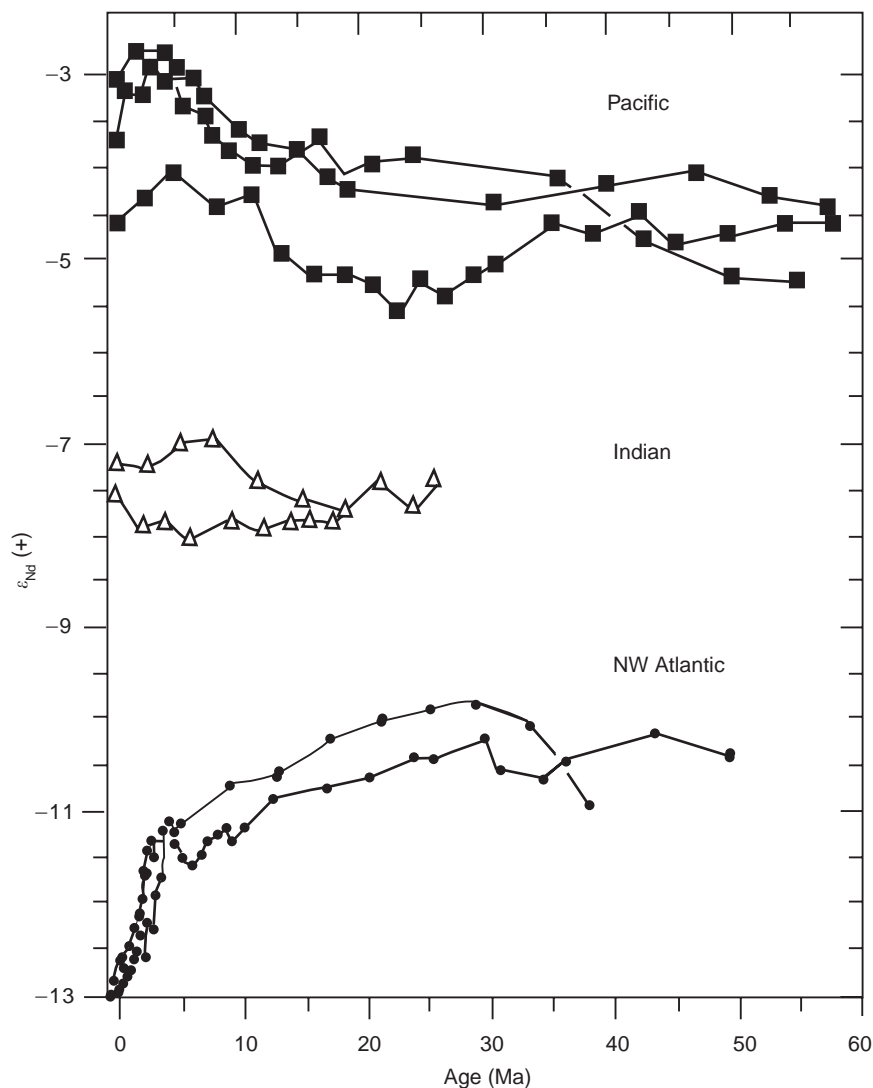


**Figure 6** Nd isotope variations in Cenozoic sea water based on the analyses of hydrogenetic Fe-Mn crusts. Note that despite the assumed  $\tau$  of more than 1000y the oceans have kept their Nd isotope provinciality observed today throughout the last 50 My. (Reprinted from *Earth and Planetary Science Letters*, 155, O'Nions RK, Frank M, von Blanckenburg F, Ling HF. Secular variations of Nd and Pb isotopes in ferromanganese crusts from the Atlantic, Indian, and Pacific Oceans, 15–28, Copyright (1998) with permission from Elsevier Science.)

circulation following the opening of the Indonesian throughways for exchange of thermocline waters, or an increase in dust input. The strong decrease in north-west Atlantic  $\epsilon_{\text{Nd}}$  over the past 3–4 My has been linked to a strengthening of NADW production following closure of the Panama gateway (suppressing northward flow of AABW and AAIW high in  $\epsilon_{\text{Nd}}$ ). However, a pronounced decrease of  $\epsilon_{\text{Nd}}$  in a shallow ferromanganese crust off Florida has occurred as early as 8–5 Ma. This has been ascribed to a decreasing inflow of Pacific water through the narrowing Panama gateway. Thus, a change in the amount and style of weathering associated with

the onset of northern hemisphere glaciation at 3 Ma is a more likely explanation for the Pleistocene decrease in  $\epsilon_{\text{Nd}}$ . In particular the Labrador Sea, a major source of NADW, is surrounded by ancient rocks with  $\epsilon_{\text{Nd}}$  as low as  $-40$  and is supplying deep water with  $\epsilon_{\text{Nd}}$  of  $-20$  to NADW (Figure 2C). An increase in weathering of this component has the potential to drive the Nd in NADW towards lower compositions.

#### Pb

No information can be obtained on natural Pb from modern sea water, because of the strong contamina-

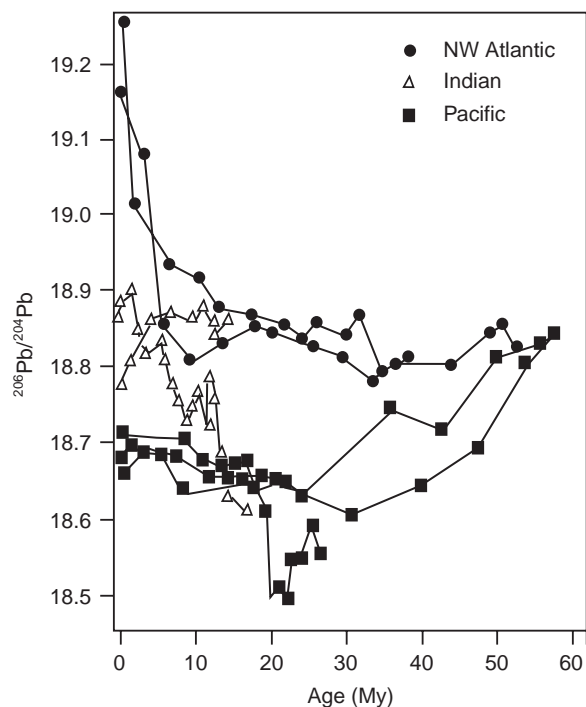


**Figure 7** Pb isotope variations in Cenozoic sea water based on the analyses of hydrogenetic Fe-Mn crusts. Because of the short  $\tau$  of Pb the oceans have maintained distinct isotope signals throughout the past 50 My. There is more intra-basin variability with time because the short  $\tau$  does not allow such efficient lateral homogenization within basins as is the case for Nd. Therefore, local changes in erosion are much more visible in Pb isotope variations. (Reprinted from *Geochimica et Cosmochimica Acta*, 63, Frank M, O'Nions RK, Hein JR, Banaker VK, 1689–1708, Copyright (1999) with permission from Elsevier Science.)

tion by industrial Pb. Therefore, the pre-anthropogenic Pb distribution has to be obtained from chemical sediments.  $^{206}\text{Pb}/^{204}\text{Pb}$  time-series, analyzed in Fe-Mn crusts (Figure 7), show patterns of changes that are less clear than those of Nd. Relative differences even within ocean basins are much larger than those observed for Nd. This may be expected from the short residence time of Pb (Table 1), which does not allow for lateral within-basin homogenization to the same degree as Nd. Therefore, local sources dominate the natural Pb budget, and their changes in flux introduce strong isotope variability. For example, in the Indian Ocean a crust located close to the circumpolar current shows a distinctly different history from the more northerly one, experiencing strong changes. The pronounced increase in north-west Atlantic  $^{206}\text{Pb}/^{204}\text{Pb}$  can be attributed, as  $\epsilon_{\text{Nd}}$ , to a change in NADW production, but is more likely due to a change in weathering of the glaciated areas or a change in the provenance of the erosional products.

## Be

$^{10}\text{Be}/^9\text{Be}$  has been analyzed in Fe-Mn crusts as chronometer for the past 10 My. The smooth logarithmic decrease in  $^{10}\text{Be}/^9\text{Be}$  (Figure 8A and C) is compatible with radioactive decay of  $^{10}\text{Be}$ . This allows for calculation of growth rates and reconstruction of the initial  $^{10}\text{Be}/^9\text{Be}$  ratios. Quite unexpectedly these initial  $^{10}\text{Be}/^9\text{Be}$  ratios have been within the present-day range of the respective ocean basins through the past 7–10 My. Since the modern ocean basins do display strongly different  $^{10}\text{Be}/^9\text{Be}$  ratios (Figure 2F), and since a  $\tau$  of *c.* 600 y favors exchange of Be between basins, the relative constancy of these ratios with time suggests that large-scale changes in deep-water circulation have not taken place within the measured period.

## Discussion and Conclusion

Changes in the style of weathering have the potential to change the isotope composition of tracers released to the sea. Leaching experiments on fresh mechanically (glacially) weathered rocks have shown a strongly incongruent release (meaning the release of tracers with varying isotope compositions depending on the mode of liberation from rocks) of radiogenic Sr, Os, and Pb, and nonradiogenic Nd (up to 16  $\epsilon_{\text{Nd}}$  units, Table 3). Strongly chemically weathered rocks do not show such an incongruent release. Therefore, some of the long-term changes seen in the isotope evolution of seawater Sr, Os, Nd, and Pb might be attributable to these effects. Certainly the evolution of Sr and Os is only controlled by weathering, and the relative contribution of various sources, such as continental rocks, MORB (Mid Ocean Ridge Basalt), carbonate recycling, peridotite weathering, and cosmic dust. The uniformity between basins makes Sr and Os isotopes reliable stratigraphic tools.

$^{10}\text{Be}/^9\text{Be}$  appears to be a robust dating tool for the past  $\sim 10$  My, due to its relatively constant observed initial ratio. It remains to be demonstrated whether Nd, Hf, and Pb have real value as tracers of past ocean circulation, as expected from their distinct water mass compositions, or whether their changes back through time merely record local changes in weathering.

Clearly the time resolution achievable from Fe-Mn crust studies is not sufficient to answer these questions. Much more insight will be obtained when these radiogenic tracers and Be isotopes are applied to sediments allowing tracer change studies at the resolution of a few thousand years. This will allow more reliable studies on the relationship between

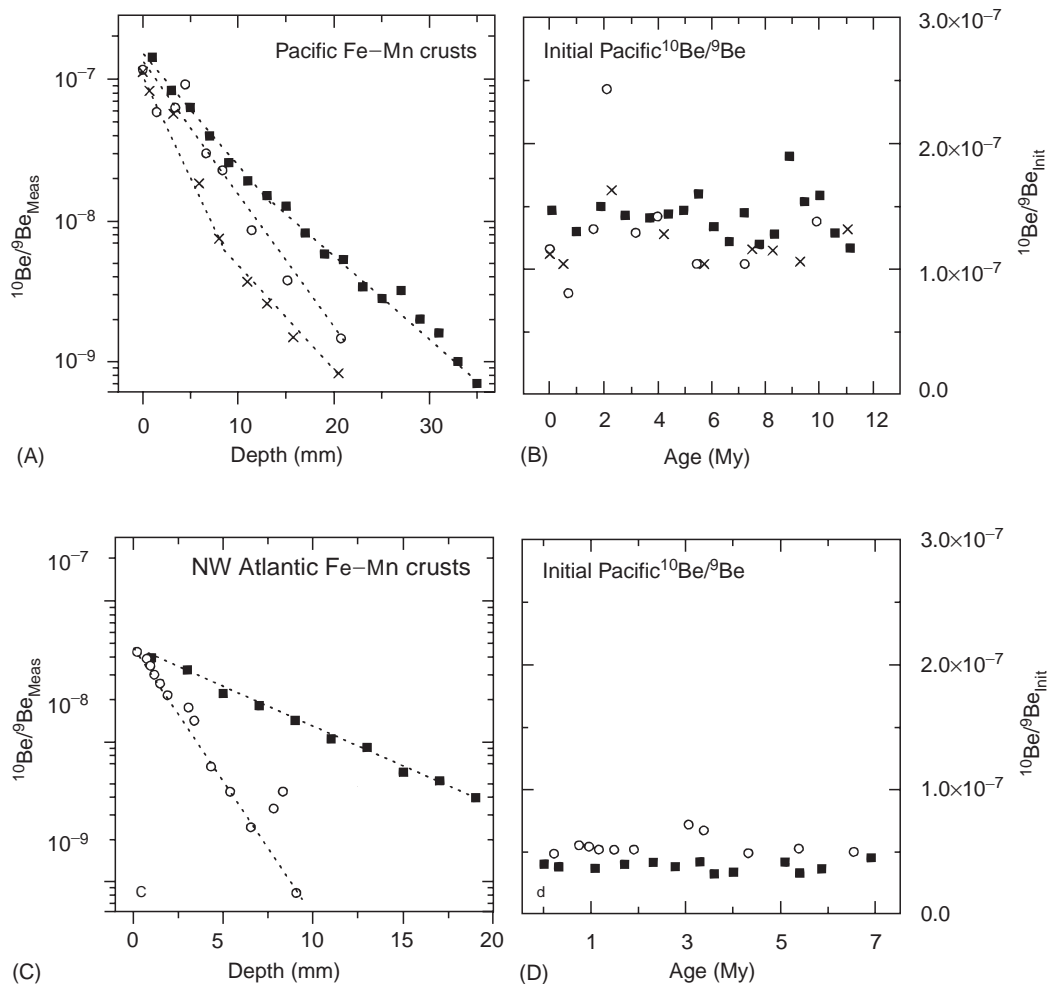


**Figure 8**  $^{10}\text{Be}/^9\text{Be}$  ratios in Pacific (A, B) and Atlantic (C, D) Fe-Mn crusts (Ling et al., 1997; von Blanckenburg and O’Nions, 1999). The smooth exponential decrease with depth usually observed in the measured data (as fitted following the stippled lines in A, C, where some individual outliers are attributed to alteration) is compatible with radioactive decay of  $^{10}\text{Be}$  only ( $T_{1/2} = 1.5$  My). A kink in the fits to the data is due to changes in growth rates. Changes in the initial ratio would be visible in the form of offsets in the data. At the time resolution of the samples taken (several hundred thousand years) these are not observed. Therefore, the derived growth rates can be used to time-correct the  $^{10}\text{Be}/^9\text{Be}$  ratios for radioactive decay and to calculate initial ratios. The results shown in B and D indicate that the  $^{10}\text{Be}/^9\text{Be}$  ratios in both the Pacific and the Atlantic have been within the range of modern sea water, for the last 7–10 My, despite presumably widely varying erosional input into the ocean.

**Table 3** Incongruent release of isotopes from strongly mechanically weathered continental rocks

Isotope ratio	Isotope change	Original fresh material	Experimental evidence
$^{87}\text{Sr}/^{86}\text{Sr}$	0.725 $\rightarrow$ 0.795	Young granitic moraine, Wind River Range, Wyoming, USA	Ammonium acetate leach River water composition HCl leach (Blum and Erel, 1995)
$^{187}\text{Os}/^{188}\text{Os}$	1.5 $\rightarrow$ 9.5	Young granitic moraine, Wind River Range, Wyoming, USA	HCl leach Young terrestrial Fe-Mn coatings Peucker-Ehrenbrink and Blum (1998)
$\epsilon_{\text{Nd}}$	-26 $\rightarrow$ -42	Greenland river bedload Baffin Bay deep-sea sediment	HCl leach (own work)
$^{206}\text{Pb}/^{204}\text{Pb}$	15.2 $\rightarrow$ 22.0	Greenland river bedload Baffin Bay deep-sea sediment	HCl and HBr leach (own work)

climate change, ocean circulation, and continental weathering.

### Suggested Reading

The topic of radiogenic seawater tracers is too novel to be covered by a single monograph. All information is spread between numerous publications in international journals. Faure (1986) gives a general introduction into radiogenic isotope techniques. Analytical methods are summarized in a monograph by Potts (1987). Broecker and Peng (1982) provide a much-cited introduction into the topic of tracers in the sea. Ferromanganese crusts have recently been summarised by Hein *et al.* (1999). McArthur (1994) has reviewed the material suitable for Sr isotope analysis in carbonates, covering all ages of deposits from recent to the Precambrian. A summary of the suitability of marine clay minerals for isotope analyses is given by Stille *et al.* (1992). A brief summary on radiogenic seawater tracers, containing useful cross-references, has been published by the author (von Blanckenburg, 1999).

### See also

**Authigenic Deposits. Carbon Cycle. Cenozoic Climate – Oxygen Isotope Evidence. Cenozoic Oceans – Carbon Cycle Models. Cosmogenic**

**Isotopes. Large Marine Ecosystems. Mid-ocean Ridge Geochemistry and Petrology. Rare Earth Elements and their Isotopes. Redfield Ratio. River Inputs. Sediment Chronologies. Stable Carbon Isotope Variations in the Ocean. Thermohaline Circulation. Tracers and Large Scale Models. Uranium–Thorium Series Isotopes in Ocean Profiles. Water Types and Water Masses.**

### Further Reading

- Broecker WS and Peng TH (1982) *Tracers in the Sea*. Palisades: Lamont-Doherty Geological Observatory.
- Faure G (1986) *Principles of Isotope Geology*. John Wiley & Sons.
- Hein JR, Koschinsky A, Bau M, Manheim FT, Kang JK and Roberts L (1999) Cobalt-rich ferromanganese crusts in the Pacific. In: Cronan DS (ed.) *Handbook of Marine Mineral Deposits*, pp. 239–279. Boca Raton: CRC Press.
- McArthur JM (1994) Recent trends in strontium isotope stratigraphy. *Terra Nova* 6: 331–358.
- Potts PJ (1987) *A Handbook of Silicate Rock Analysis*. Blackie.
- Stille P, Chaudhuri S, Kharaka YK and Clauer N (1992) Neodymium, strontium, oxygen and hydrogen isotope compositions of waters in present and past oceans: a review. In: Clauer N and Chaudhuri S (eds.) *Isotopic Signatures and Sedimentary Rocks*, p. 555. Berlin: Springer Verlag.
- von Blanckenburg F (1999) Tracing past ocean circulation? *Science* 286: 1862–1863.